

Dragging of inertial frames inside the rotating neutron stars

Chandrachur Chakraborty, Kamakshya Prasad Modak, Debades Bandyopadhyay

*Astroparticle Physics and Cosmology Division
Saha Institute of Nuclear Physics, Kolkata 700064, India*

chandrachur.chakraborty@saha.ac.in

kamakshya.modak@saha.ac.in

ABSTRACT

We derive the exact frame-dragging rate inside the rotating neutron star. This formula is applied to obtain the frame-dragging frequency at the centre of this object precisely. Using this formulation we show that the frame-dragging rate monotonically decreases from the centre to the surface of the pole. But there appears an anomaly in the frame-dragging rate from the centre to the surface of the equator and its around. Moving from the equator to the pole, this anomaly disappears after crossing a certain ‘critical’ angle. It is also shown that this anomaly is completely independent of the equations of state and it depends only on the rotation frequency and the central density of a particular pulsar.

1. Introduction

Stationary spacetimes with angular momentum (rotation) are known to exhibit an effect whereby the locally inertial frames are dragged along the rotating spacetime, making any test particle in such spacetimes precess with a certain frequency called the frame-dragging frequency or the Lense-Thirring (LT) precession frequency (Ω_{LT}). The LT frequency for a test particle has been calculated and shown to fall with the inverse cube of the distance of the test particle from the source for large enough distances where the curvature effects are small. It is also proportional to the angular momentum of the source. The precession frequencies are thus expected to be very large for a distance near the source (like the surface and interior of a neutron star or a pulsar, or near the horizon of a black hole) as well as for spacetimes rotating very fast with large angular momenta.

Pulsars are compact and much more massive ($1M_{\odot} < M < 2 - 3M_{\odot}$) objects than the Sun. Many of them are observed to possess very high angular velocities. Hence the spacetime curvature is much higher in the nearby surroundings for their masses. The dragging frequencies of inertial frames are thus very much effective for strong gravity calculations of the LT precession rates of the pulsars. The inertial frames are dragged not only outside the pulsars but also inside the rotating neutron stars. Basically, the frame-dragging frequency in the interior of the pulsar is much more higher than the outside frame-dragging frequency. The frame-dragging frequency is increasing more and more as one proceeds from the surface to the centre ($r = 0$) of the pulsar. This rate is maximum at the centre ($r = 0$) of the pulsar but the maximum precession rate $\Omega_{LT}(r = 0)$ will not be greater than the frequency of the pulsar Ω . The above stated condition can be mathematically expressed as $\Omega_{LT}(r = 0) \leq \Omega$.

A very first approach to give a theoretical prescription to determine the rate of the frame-dragging precession inside the rotating neutron star has been done by Hartle (Hartle 1967). By the virtue of this formalism, one can estimate roughly the frame-dragging precession rate inside a rotating neutron star. But this formalism lacks proper analytic solution inside a rotating star by which one can exactly determine the precession rate at any distance r and any angle θ . The final expression of frame-dragging precession rate depends solely on r , the distance from the centre of the star as in Hartle’s formalism. But inside the rotating objects, one should not a priori expect to observe the similar variation of the precession rates along the equatorial and polar plane. Moreover we never get the same precession rates in the equator and the pole for the same test particle which is rotating around a massive object in a fixed radius. Thus a dependency of the frame-dragging frequency on the colatitude (θ) of the position of the test particle should arise, which did not arise in the previous formalism

proposed by Hartle. Even we know that the LT precession must depends on both the radial distance (r) and the colatitude (θ) (see Eq.(14.34) of (Hartle 2009)) in very weak gravitational fields (far away from the surface of the rotating object) also. Thus, the only r dependency of frame dragging frequency inside the rotating neutron star may be questionable (even it rotates slow).

Our main motivation of this paper lies in computing the exact LT precession rates inside the rotating neutron star. In some previous literatures the formalism for calculating the LT precession rate accurately for both weak and strong gravity cases has been developed. The exact Lense-Thirring precession rate in strongly curved stationary spacetime has been discussed in detail by Chakraborty and Majumdar (Chakraborty & Majumdar 2014). Later, Chakraborty and Pradhan (Chakraborty & Pradhan 2013) applied this formulation in various stationary and axisymmetric spacetimes.

To make this more clear we have to avoid all type of approximations and assumptions to obtain the exact LT precession rate inside the rotating neutron stars. It could be seen that the exact value of LT precession rate in the center of a neutron star had been chosen arbitrarily (see page 370 of (Weber 1999)). We try to give an exact expression of the LT precession rate at the center of a pulsar and from that expression we can easily calculate numerically the value of the precession rate at the center for any known pulsar.

The paper is accordingly organized as follows. In section 2 we present the basic equations of frame-dragging effect inside the rotating neutron stars. The numerical method, which has been followed in the whole paper, is discussed in section 3. We thoroughly discuss our results in section 4. Finally we conclude in section 5 with a summary and a discussion on future outlook.

2. Basic equations of frame-dragging effect inside the rotating neutron stars

The rotating equilibrium models considered in this paper are stationary and axisymmetric. Thus we can write the metric inside the rotating neutron star as the following Komatsu-Eriguchi-Hachisu (KEH) (Komatsu et. al. 1989) form:

$$ds^2 = -e^{\gamma+\sigma} dt^2 + e^{2\alpha} (dr^2 + r^2 d\theta^2) + e^{\gamma-\sigma} r^2 \sin^2 \theta (d\phi - \omega dt)^2 \quad (1)$$

where $\gamma, \sigma, \alpha, \omega$ are the functions of r and θ only. In the whole paper we have used the geometrized unit ($G = c = 1$). We assume that the matter source is a perfect fluid with a stress-energy tensor given by

$$T^{\mu\nu} = (\rho_0 + \rho_i + P)u^\mu u^\nu + P g^{\mu\nu} \quad (2)$$

where ρ_0 is the rest energy density, ρ_i is the internal energy density, P is the pressure and u^μ is the matter four velocity. We are further assuming that there is no meridional circulation of the matter so that the four-velocity u^μ is simply a linear combination of time and angular Killing vectors. Now, we have to calculate the frame-dragging rate based on the above metric and this will gives us the exact frame-dragging rate inside a rotating neutron star.

We know that the vector field corresponding to the LT precession co-vector can be expressed as

$$\Omega = \frac{1}{2} \frac{\epsilon_{ijl}}{\sqrt{-g}} \left[g_{0i,j} \left(\partial_l - \frac{g_{0l}}{g_{00}} \partial_0 \right) - \frac{g_{0i}}{g_{00}} g_{00,j} \partial_l \right] \quad (3)$$

For the axisymmetric spacetime, the only non-vanishing component is $g_{0i} = g_{0\phi}$, $i = \phi$ and $j, l = r, \theta$; substituting these in eq. (3), the LT precession frequency vector is obtained as:

$$\Omega_{LT} = \frac{1}{2\sqrt{-g}} \left[\left(g_{0\phi,r} - \frac{g_{0\phi}}{g_{00}} g_{00,r} \right) \partial_\theta - \left(g_{0\phi,\theta} - \frac{g_{0\phi}}{g_{00}} g_{00,\theta} \right) \partial_r \right] \quad (4)$$

As the above expression has been expressed in the co-ordinate basis we have to convert it into the orthonormal basis. Thus, in the orthonormal ‘Copernican’ basis at rest in the rotating spacetime, with our choice of polar co-ordinates, $\vec{\Omega}_{LT}$ can be written as (Chakraborty & Majumdar 2014)

$$\vec{\Omega}_{LT} = \frac{1}{2\sqrt{-g}} \left[\sqrt{g_{rr}} \left(g_{0\phi,\theta} - \frac{g_{0\phi}}{g_{00}} g_{00,\theta} \right) \hat{r} + \sqrt{g_{\theta\theta}} \left(g_{0\phi,r} - \frac{g_{0\phi}}{g_{00}} g_{00,r} \right) \hat{\theta} \right] \quad (5)$$

where $\hat{\theta}$ is the unit vector along the direction θ and \hat{r} is the unit vector along the direction r . We note that the above formulation is valid only in the timelike spacetimes, not in the lightlike or spacelike regions.

Now, we can apply the above Eq.(5) to determine the exact frame-dragging rate inside the rotating neutron star of which the metric could be determined from the line-element(1). The various metric components can be read off from the metric. Likewise,

$$\sqrt{-g} = r^2 e^{2\alpha+\gamma} \sin \theta \quad (6)$$

In orthonormal coordinate basis, the exact Lense-Thirring precession rate inside the rotating neutron star is:

$$\Omega_{LT} = \frac{e^{-(\alpha+\sigma)}}{2(\omega^2 r^2 \sin^2 \theta - e^{2\sigma})}. \quad (7)$$

$$\left[\sin \theta [r^3 \omega^2 \omega_{,r} \sin^2 \theta + e^{2\sigma} (2\omega + r\omega_{,r} - 2\omega r\sigma_{,r})] \hat{\theta} + [r^2 \omega^2 \omega_{,\theta} \sin^3 \theta + e^{2\sigma} (2\omega \cos \theta + \omega_{,\theta} \sin \theta - 2\omega \sigma_{,\theta} \sin \theta)] \hat{r} \right]$$

and the modulus of the above LT precession rate is

$$|\Omega_{LT}(r, \theta)| = \frac{e^{-(\alpha+\sigma)}}{2(\omega^2 r^2 \sin^2 \theta - e^{2\sigma})}. \quad (8)$$

$$[\sin^2 \theta [r^3 \omega^2 \omega_{,r} \sin^2 \theta + e^{2\sigma} (2\omega + r\omega_{,r} - 2\omega r\sigma_{,r})]^2 + [r^2 \omega^2 \omega_{,\theta} \sin^3 \theta + e^{2\sigma} (2\omega \cos \theta + \omega_{,\theta} \sin \theta - 2\omega \sigma_{,\theta} \sin \theta)]^2]^{\frac{1}{2}}$$

Following KEH we can write the general relativistic field equations determining σ, γ and ω as

$$\Delta \left[\sigma e^{\frac{\gamma}{2}} \right] = S_\sigma(r, \mu) \quad (9)$$

$$\left(\Delta + \frac{1}{r} \partial_r - \frac{\mu}{r^2} \partial_\mu \right) \left[\gamma e^{\frac{\gamma}{2}} \right] = S_\gamma(r, \mu) \quad (10)$$

$$\left(\Delta + \frac{2}{r} \partial_r - \frac{2\mu}{r^2} \partial_\mu \right) \left[\omega e^{\frac{\gamma}{2}-\sigma} \right] = S_\omega(r, \mu) \quad (11)$$

where

$$\Delta \equiv \partial_r^2 + \frac{2}{r} \partial_r + \frac{1-\mu^2}{r^2} \partial_\mu^2 - \frac{2\mu}{r^2} \partial_\mu + \frac{1}{r^2(1-\mu^2)} \partial_\phi^2 \quad (12)$$

is the flat-space spherical coordinate Laplacian, $\mu = \cos \theta$ and $S_\sigma, S_\gamma, S_\omega$ are the effective source terms that include the nonlinear and coupling terms. The effective source terms are given by

$$\begin{aligned} S_\sigma(r, \mu) = & e^{\gamma/2} \left\{ 8\pi(\rho_0 + \rho_i + P) e^{2\alpha} \frac{1+v^2}{1-v^2} + r^2(1-\mu^2) e^{-2\sigma} \left[\omega_{,r}^2 + \frac{1-\mu^2}{r^2} \omega_{,\mu}^2 \right] + \frac{1}{r} \gamma_{,r} - \frac{\mu}{r^2} \gamma_{,\mu} \right. \\ & \left. + \frac{\sigma}{2} \left[16\pi P e^{2\alpha} - \frac{1}{r} \gamma_{,r} + \frac{\mu}{r^2} \gamma_{,\mu} - \frac{1}{2} \gamma_{,r}^2 - \frac{1-\mu^2}{2r^2} \gamma_{,\mu}^2 \right] \right\}, \end{aligned} \quad (13)$$

$$S_\gamma(r, \mu) = e^{\gamma/2} \left[16\pi e^{2\alpha} P + \frac{\gamma}{2} \left(16\pi e^{2\alpha} P - \frac{1}{2} \gamma_{,r}^2 - \frac{1-\mu^2}{2r^2} \gamma_{,\mu}^2 \right) \right], \quad (14)$$

$$\begin{aligned} S_\omega(r, \mu) = & e^{\gamma/2-\sigma} \left\{ -16\pi \frac{(\rho_0 + \rho_i + P)(\Omega - \omega)}{1-v^2} e^{2\alpha} + \omega \left[-8\pi \frac{(\rho_0 + \rho_i)(1+v^2) + 2Pv^2}{1-v^2} e^{2\alpha} - \frac{1}{r} \left(\frac{1}{2} \gamma_{,r} + 2\sigma_{,r} \right) \right. \right. \\ & \left. \left. + \frac{\mu}{r^2} \left(\frac{1}{2} \gamma_{,\mu} + 2\sigma_{,\mu} \right) + \sigma_{,r}^2 - \frac{1}{4} \gamma_{,r}^2 + \frac{1-\mu^2}{4r^2} (\gamma_{,\mu}^2 + 4\sigma_{,\mu}^2) - r^2(1-\mu^2) e^{-2\sigma} \left(\omega_{,r}^2 + \frac{1-\mu^2}{r^2} \omega_{,\mu}^2 \right) \right] \right\}. \end{aligned} \quad (15)$$

where Ω is the angular velocity of the matter as measured at infinity and v is the proper velocity of the matter with respect to a zero angular momentum observer. The proper velocity of the matter is given by

$$v = (\Omega - \omega) r e^{-\sigma} \sin \theta \quad (16)$$

and the coordinate components of the four-velocity of the matter can be written as

$$u^\mu = \frac{e^{-(\sigma+\gamma)/2}}{\sqrt{1-v^2}}[1, 0, 0, \Omega] \quad (17)$$

We obtain two first order partial differential equations for the metric function α . However, in the numerical method to determine α we need only one of them, namely the following

$$\begin{aligned} \alpha_{,\mu} = & -\frac{1}{2}(\gamma_{,\mu} + \sigma_{,\mu}) - \left\{ (1 - \mu^2)(1 + r\gamma_{,r})^2 + [\mu(1 - \mu^2)\gamma_{,\mu}]^2 \right\}^{-1} \\ & \left\{ \frac{1}{2} [r^2(\gamma_{,rr} + \gamma_{,r}^2) - (1 - \mu^2)(\gamma_{,\mu}^2 + \gamma_{,\mu\mu})] [-\mu + (1 - \mu^2)\gamma_{,\mu}] + \frac{3}{2}\mu\gamma_{,\mu}[-\mu + (1 - \mu^2)\gamma_{,\mu}] \right. \\ & + \frac{1}{4}[-\mu + (1 - \mu^2)\gamma_{,\mu}] [r^2(\gamma_{,r} + \sigma_{,r})^2 - (1 - \mu^2)(\gamma_{,\mu} + \sigma_{,\mu})^2] + r\gamma_{,r} \left[\frac{\mu}{2} + \mu r\gamma_{,r} + \frac{(1 - \mu^2)\gamma_{,\mu}}{2} \right] \\ & \left. - (1 - \mu^2)r(1 + r\gamma_{,r}) \left[\gamma_{,r\mu} + \gamma_{,\mu}\gamma_{,r} + \frac{1}{2}(\gamma_{,\mu} + \sigma_{,\mu})(\gamma_{,r} + \sigma_{,r}) \right] + \frac{1}{4}(1 - \mu^2)e^{-2\sigma} \right. \\ & \left. [r^4\mu\omega_{,r}^2 + (1 - \mu^2)[2r^3\omega_{,r}\omega_{,\mu} - \mu r^2\omega_{,\mu}^2 + 2r^4\gamma_{,r}\omega_{,r}\omega_{,\mu}] - r^2(1 - \mu^2)\gamma_{,\mu}[r^2\omega_{,r}^2 - (1 - \mu^2)\omega_{,\mu}^2]] \right\} \quad (18) \end{aligned}$$

We can obtain the LT precession rate

$$|\Omega_{LT}|_{r=0} = \omega e^{-(\alpha+\sigma)}|_{r=0} \quad (19)$$

at the center ($r = 0$) of a rotating neutron star.

3. Numerical method

Here we adopt the rotating neutron star (**rns**) code based on the KEH ([Komatsu et. al. 1989](#)) method and written by Stergioulas ([Stergioulas 1995](#)) to obtain the frame-dragging rate inside the rotating neutron stars. The equations for the gravitational and matter fields were solved on a discrete grid using a combination of integral and finite difference techniques. The computational domain of the problem is $0 \leq r \leq \infty$ and $0 \leq \mu \leq 1$. It is easy to deal with finite radius rather than the infinite domain with via a coordinate transformation to a new radial coordinate s which covers the infinite radial span in a finite coordinate interval $0 \leq s \leq 1$. This new radial coordinate s is defined by

$$r = r_e \cdot \frac{s}{1 - s} \quad (20)$$

Thus, $s = \frac{1}{2}$ represents the radius of the equator (r_e) of the pulsar and $s = 1$ represents the infinity. The three elliptical field equations (9)-(11) were solved by an integral Green's function approach following the KEH. Taking into account the equatorial and axial symmetry in the configurations we can find the three metric

coefficients ρ, γ, ω which can be written as

$$\begin{aligned} \rho(s, \mu) = & -e^{-\frac{\gamma}{2}} \sum_{n=0}^{\infty} P_{2n}(\mu) \left[\left(\frac{1-s}{s} \right)^{2n+1} \int_0^s \frac{s'^{2n} ds'}{(1-s')^{2n+2}} \int_0^1 d\mu' P_{2n}(\mu') \bar{S}_\rho(s', \mu') \right. \\ & \left. + \left(\frac{s}{1-s} \right)^{2n} \int_s^1 \frac{(1-s')^{2n-1} ds'}{s'^{2n+1}} \int_0^1 d\mu' P_{2n}(\mu') \bar{S}_\rho(s', \mu') \right], \end{aligned} \quad (21)$$

$$\begin{aligned} \gamma(s, \mu) = & -\frac{2e^{-\frac{\gamma}{2}}}{\pi} \sum_{n=1}^{\infty} \frac{\sin[(2n-1)\theta]}{(2n-1)\sin\theta} \left[\left(\frac{1-s}{s} \right)^{2n} \int_0^s \frac{s'^{2n-1} ds'}{(1-s')^{2n+1}} \int_0^1 d\mu' \sin[(2n-1)\theta'] \bar{S}_\gamma(s', \mu') \right. \\ & \left. + \left(\frac{s}{1-s} \right)^{2n-2} \int_s^1 \frac{(1-s')^{2n-3} ds'}{s'^{2n-1}} \int_0^1 d\mu' \sin[(2n-1)\theta'] \bar{S}_\gamma(s', \mu') \right], \end{aligned} \quad (22)$$

$$\begin{aligned} \hat{\omega}(s, \mu) \equiv r_e \omega(s, \mu) = & -e^{(\rho-\frac{\gamma}{2})} \sum_{n=1}^{\infty} \frac{P_{2n-1}^1(\mu)}{2n(2n-1)\sin\theta} \left[\left(\frac{1-s}{s} \right)^{2n+1} \int_0^s \frac{s'^{2n} ds'}{(1-s')^{2n+2}} \int_0^1 d\mu' \sin\theta' P_{2n-1}^1(\mu') \bar{S}_\omega(s', \mu') \right. \\ & \left. + \left(\frac{s}{1-s} \right)^{2n-2} \int_s^1 \frac{(1-s')^{2n-3} ds'}{s'^{2n-1}} \int_0^1 d\mu' \sin\theta' P_{2n-1}^1(\mu') \bar{S}_\omega(s', \mu') \right]. \end{aligned} \quad (23)$$

where $P_n(\mu)$ are the Legendre polynomials and $P_n^m(\mu)$ are the associated Legendre polynomials and $\sin(n\theta)$ is a function of μ through $\theta = \cos^{-1} \mu$. The effective sources could be defined as

$$\bar{S}_\rho(s, \mu) = r^2 S_\rho(s, \mu) \quad (24)$$

$$\bar{S}_\gamma(s, \mu) = r^2 S_\gamma(s, \mu) \quad (25)$$

$$\bar{S}_\omega(s, \mu) = r_e r^2 S_\omega(s, \mu) \quad (26)$$

The advantages of this Green's function approach for solving the elliptic field equations is that the asymptotic conditions on ρ, γ, ω are imposed automatically. The numerical integration of the Eqs. (21)-(23) is straightforward. These integrations are solved using the **rns** code and we obtain the value of frame-dragging precession rate inside the rotating neutron star using the equation (8).

3.1. Equation of state (EoS) of dense matter

Recent observations of PSR J0348+0432 reported the measurement of a 2.01 ± 0.04 pulsar (Antoniadis et al. 2013). This is the most accurately measured highest neutron star mass so far. The accurately measured neutron star mass is a direct probe of dense matter in its interior. This measured mass puts the strong constraint on the EoS.

Equations of state of dense matter are used as inputs in the calculation of frame-dragging in neutron star interior. We adopt three equations of state in this calculation. We are considering equations of state of β -equilibrated nuclear matter. The chiral EoS is based on the QCD motivated chiral $SU(3)_L \times SU(3)_R$ model (Hanauske et al. 2000). We exploit the density dependent (DD) relativistic mean model to construct the DD2 EoS (Typel et al. 2010). Here the nucleon-nucleon interaction is mediated by the exchange of mesons and the density dependent nucleon-meson couplings are obtained by fitting properties of finite nuclei. The other EoS is the Akmal, Pandharipande and Ravenhall (APR) EoS calculated in the variational chain summation method using Argonne V_{18} nucleon-nucleon interaction and a fitted three nucleon interaction along with relativistic boost corrections (Akmal et al. 1998).

We calculate the static mass limits of neutron stars using those three equations of state. The maximum masses and the corresponding radii of neutron stars are recorded in Table 1. These results show that maximum masses in all three cases are above $2 M_\odot$ and compatible with the benchmark measurement mentioned above.

4. Results

We divide our results into two sections: in the first section we show the frame-dragging effect of some pulsars which rotate with their Kepler frequencies Ω_k and central densities ε_c remain fixed. In the next section

we take some real pulsars which exist in our universe. The mass M and rotational frequency Ω are fixed in these cases but the pulsars do not rotate with their Kepler frequencies. Their rotational frequencies are generally much lower than their Kepler frequencies ($\Omega < \Omega_k$).

4.1. Pulsars rotate with their own Kepler frequencies $\Omega = \Omega_k$

It could be easily seen from the Eq.(8) that the frame-dragging frequency inside a neutron star could not be a function of only the radial distance r but also of the colatitude θ . The colatitude takes a major role to determine the exact frame-dragging frequency at a particular point inside the rotating neutron star. The dragging frequencies as a function of radial distance (from the star's centre to its surface) and colatitude are exhibited for several sample star in Figures 1-3 with three equations of state.

In each figure the masses of these stars are increasing from ~ 0.6 to ~ 1.2 to $\sim 1.7M_\odot$ with the increase of the central density ε_c . The angular velocities Ω and Ω_{LT} are measured by the distant observer. The rotational frequency of each stellar model is the Kepler frequency, Ω_k and the values correspond to Kepler periods of $P_k = 1.57$ ms, 1.26 ms and 1.05 ms. According to the theorem by Hartle, the dragging of inertial frames with respect to a distant observer is always greater at the star's center, where the mass-energy density is the largest, and is decreasing in the radial outward direction. Both features are confirmed in Figs.1-3. The smooth behaviour of $\bar{\omega}/\Omega$ as a function of r and θ is typical for a stable star configuration. Otherwise, the dragging of the local inertial frames would be sharply peaked. The relative frame-dragging values at the center and the surface of the star models shown in these figures are listed in the table: It is noted that $\tilde{\omega}_c \approx 51 - 88\%$ at the star's center and falls off to $\tilde{\omega}_s \approx 3 - 7\%$ on the surface of the equator and $\tilde{\omega}_s \approx 15 - 28\%$ on the surface of the pole for the highest central density and the smallest Kepler period, $P_k = 1.05$ ms. Furthermore smaller values of $\tilde{\omega}_c \approx 24 - 35\%$ at the star's center and falls off to $\tilde{\omega}_s \approx 1 - 2\%$ at the surface of the equator and $\tilde{\omega}_s \approx 5 - 10\%$ at the surface of the pole are obtained in less dense stars rotating at $P_k = 1.57$ ms. One can see another interesting thing from the Table 2 that $\tilde{\omega}_s$ is always higher at the pole than $\tilde{\omega}_s$ at the equator for a particular pulsar. It is due to the effect of rotation frequency Ω (of the star) for which pole is nearer to the center than the surface as it is evident from Table 2. Thus, the inertial frame-dragging effect is higher at the surface of the pole than the surface of the equator.

It could be easily seen from Figs.1-3 that the plots are smooth along the pole but not along the equator. We can see that there exists an anomaly: the 'peak' and 'dip' take place in the plots along the equator. These are absent in the Hartle's formulation((Hartle 1967), (Weber 1999)). In this formalism the frame-dragging frequency depends solely on r but not on θ . So, they get the same frequency (for a fixed r) in everywhere (from the equator to the pole) inside the rotating neutron star. In our case, frame-dragging does not depend only on r but also on colatitude θ . Thus, the frame-dragging frequency could not be the same everywhere for a fixed radius r . The figures show that the frame-dragging along the equator tends to zero (very low frequency but not almost zero) around $r_{peak} \approx 0.5r_e$ and it increases again to achieve its second 'maximum' around $r_{dip} \approx 0.7r_e$. After this 'dip', the frame-dragging frequency decreases very fast and vanishes at infinity. As the rotation frequency Ω_k and the central energy density ε_c increase, the frame-dragging frequency increases and also the 'peak' and the 'dip' shift towards the surface of the equator for all EoSs. It reveals an important

| EoS | P(ms) | $\varepsilon_c(10^{15} \text{ g/cm}^3)$ | M_G/M_\odot | R (km) |
|--------|--------|---|---------------|----------|
| APR | static | 2.78 | 2.190 | 9.93 |
| | 0.6291 | 1.50 | 2.397 | 14.53 |
| DD2 | static | 1.94 | 2.417 | 11.90 |
| | 0.7836 | 1.00 | 2.677 | 17.53 |
| Chiral | static | 1.99 | 2.050 | 12.14 |
| | 0.8778 | 1.11 | 2.353 | 18.17 |

Table 1: Maximum gravitational masses (M_G/M_\odot), equatorial radii (R), and their corresponding central energy densities (ε_c) for static ($\Omega = 0$) and Keplerian limit ($P = P_k = 2\pi/\Omega_k$) with different EoS, where P_k is the Kepler period in millisecond.

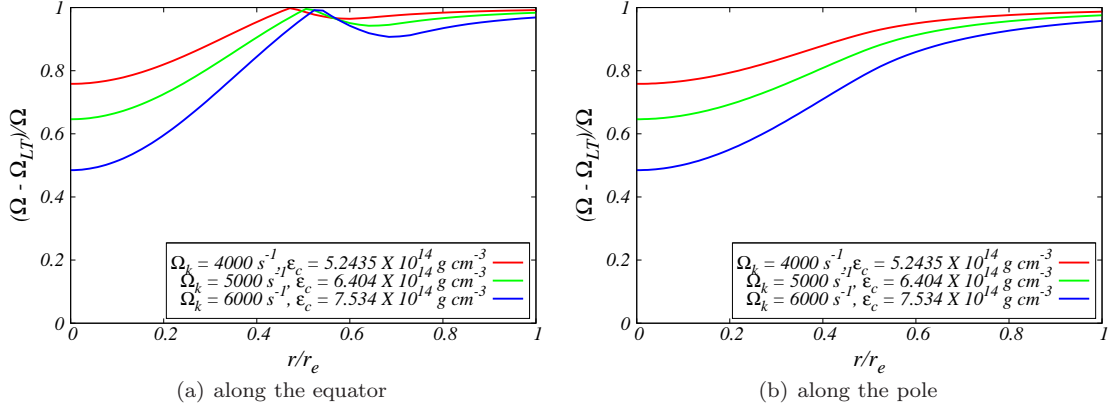


Fig. 1.— *Frame-dragging effect inside the rotating neutron stars from the origin to the surface, calculated for the APR EoS. Ω_k and ϵ_c denote the Kepler frequency and the central star density, respectively. Surface of the pole located around $0.6r_e$ but the plot is still valid beyond the surface of the pole as our formalism is applicable for regions outside the pulsar.*

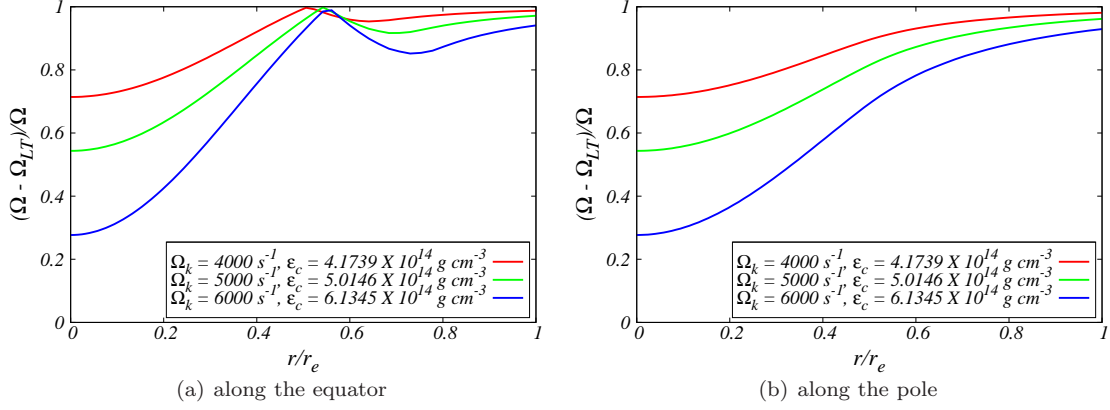


Fig. 2.— *Same as Fig. 1, but calculated for the DD2 EoS*

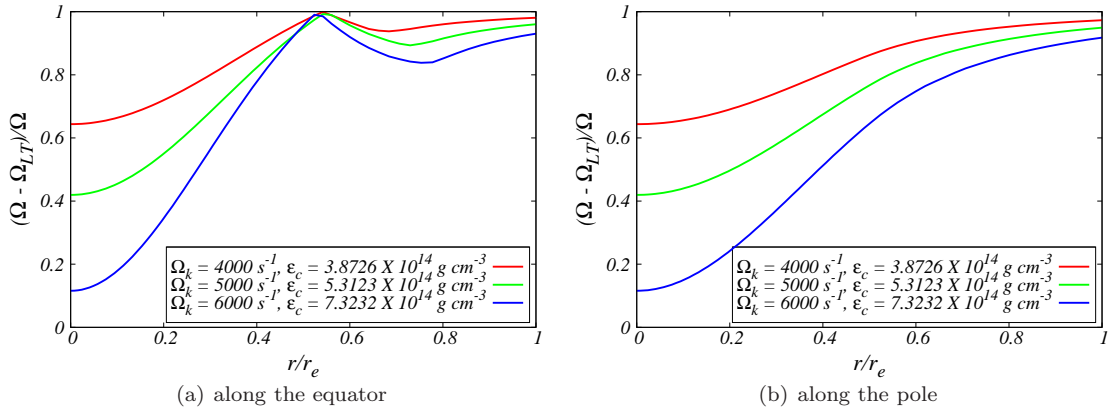


Fig. 3.— *Same as Fig. 1, but calculated for the Chiral EoS.*

conclusion that *the position of the ‘peak’ and the ‘dip’ must depend on Ω and ε_c for a particular pulsar*. This conclusion could also be drawn from Fig.4 with DD2 and APR EoS. In this figure panel (a) is plotted for Ω_{LT} as a function of s and $\cos\theta$ for the DD2 EoS and same thing is plotted due to APR EoS in panel (b). The plots along the pole have the clear pictures, frame-dragging frequency decreases from center to the surface of the pole. As latitude ($\theta' = \pi/2 - \theta$) increases from the equator to the pole, the ‘heights’ of the ‘peak’ and the ‘dip’ decrease and after a certain ‘critical’ angle (θ_{cr}) both of them disappear and the plot is smooth like the plot along the pole. The critical angle could be seen from the 3-D plot in Fig.4. It is generally near about $\mu \approx 0.5$ or $\theta'_{cr} = 30^\circ$ where both of them, i.e., ‘peak’ and ‘dip’ disappear. So, if we plot Ω_{LT} vs θ at the point r_{peak} for one case, (namely when $\Omega_k = 5000 \text{ s}^{-1}$), we can see that the frame-dragging frequency increases from the equator to the pole for the specific r_{peak} (it is also clear from Fig.4). Thus, the two different plots of a particular pulsar (rotating with $\Omega_k = 5000 \text{ s}^{-1}$, Fig.4) compel us to take another major conclusion that *the value of θ_{cr} is independent EoSs for a particular pulsar*.

We can also plot the frame-dragging frequency outside the rotating neutron stars, we mean from the center of the neutron star to the infinity but we are not interested here. The frame-dragging frequency repeatedly falls outside the rotating neutron star. So, it is not too much interesting as it is very well-known at present. Our main focus is only the interior of the rotating neutron star. One should ask that why we are getting the ‘peak’ and ‘dip’ for the plots along the equator and its nearby regions. To find out the mystery we differentiate Eq.(8) with respect to r and we obtain

$$\begin{aligned} \frac{d\Omega_{LT}}{dr} &= \Omega_{LT} \left[-(\alpha_{,r} + \sigma_{,r}) - 2 \frac{r\omega \sin^2 \theta (r\omega_{,r} + \omega) - \sigma_{,r} e^{2\sigma}}{\omega^2 r^2 \sin^2 \theta - e^{2\sigma}} \right] + \frac{1}{\Omega_{LT}} \cdot \frac{e^{-2(\alpha+\sigma)}}{4(\omega^2 r^2 \sin^2 \theta - e^{2\sigma})^2} \\ &\cdot \left\{ A \sin^2 \theta [\omega r^2 \sin^2 \theta (3\omega\omega_{,r} + 2r\omega_{,r}^2 + r\omega\omega_{,rr}) + 2\sigma_{,r} e^{2\sigma} (2\omega + r\omega_{,r} - 2\omega r\sigma_{,r}) \right. \\ &+ e^{2\sigma} (3\omega_{,r} + r\omega_{,rr} - 2r\omega_{,r}\sigma_{,r} - 2\omega\sigma_{,r} - 2r\omega\sigma_{,rr})] + B [r\omega \sin^3 \theta (2\omega\omega_{,\theta} + 2r\omega_{,r}\omega_{,\theta} + r\omega\omega_{,\theta r}) \\ &+ 2\sigma_{,r} e^{2\sigma} (2\omega \cos \theta + \omega_{,\theta} \sin \theta - 2\omega\sigma_{,\theta} \sin \theta) + e^{2\sigma} (2\omega_{,r} \cos \theta + \omega_{,\theta r} \sin \theta - 2 \sin \theta (\omega\sigma_{,\theta r} + \omega_{,r}\sigma_{,\theta})) \left. \right\} \end{aligned} \quad (27)$$

in where

$$A = r^3 \omega^2 \omega_{,r} \sin^2 \theta + e^{2\sigma} (2\omega + r\omega_{,r} - 2\omega r\sigma_{,r}) , \quad (28)$$

$$B = r^2 \omega^2 \omega_{,\theta} \sin^3 \theta + e^{2\sigma} (2\omega \cos \theta + \omega_{,\theta} \sin \theta - 2\omega\sigma_{,\theta} \sin \theta) \quad (29)$$

and

$$\omega_{,\theta r} \equiv \frac{\partial^2 \omega}{\partial \theta \partial r}$$

Setting $\frac{d\Omega_{LT}}{dr}|_{r=R_0} = 0$ and solving it numerically in the region $0 < R_0 < r_e$, we obtain two positive real roots of r inside the rotating neutron star. One of these is $R_{01} = r_{peak}$ and another is $R_{02} = r_{dip}$. The following conditions are also satisfied, namely,

$$\frac{d^2 \Omega_{LT}}{dr^2}|_{r=r_{peak}} > 0 \quad \text{and} \quad \frac{d^2 \Omega_{LT}}{dr^2}|_{r=r_{dip}} < 0 \quad (30)$$

| | P_k (ms) | Along the equator | | | Along the pole | | |
|--------------------|---------------|-------------------|-------|--------|----------------|-------|--------|
| | | APR | DD2 | Chiral | APR | DD2 | Chiral |
| $\tilde{\omega}_s$ | 1.57 | 0.008 | 0.013 | 0.019 | 0.046 | 0.069 | 0.099 |
| | 1.26 | 0.016 | 0.029 | 0.040 | 0.087 | 0.139 | 0.184 |
| | 1.05 | 0.031 | 0.059 | 0.070 | 0.151 | 0.252 | 0.287 |
| $\tilde{\omega}_c$ | 1.57 | 0.242 | 0.286 | 0.356 | 0.242 | 0.286 | 0.356 |
| | 1.26 | 0.354 | 0.457 | 0.580 | 0.354 | 0.457 | 0.580 |
| | 1.05 | 0.515 | 0.723 | 0.884 | 0.515 | 0.723 | 0.884 |

Table 2: Relative angular velocities of the local inertial frame-dragging at the surface $\tilde{\omega}_s (\equiv \omega_s/\Omega_k)$ and the centre $\tilde{\omega}_c (\equiv \omega_c/\Omega_k)$ of the neutron stars which are rotating at their respective Kepler periods ($P_k \equiv 2\pi/\Omega_k$) which are measured by a distant observer.

4.2. Pulsars rotate with their frequencies $\Omega < \Omega_k$

Generally, the real pulsars do not rotate with their specific Kepler frequencies. Their exact rotational frequencies are much lower than their respective Kepler frequencies, so that the ratio between r_p/r_e is not to be less than 0.9. But, this does not mean that the frame-dragging precession rates are not much higher in the cases of real pulsars. Due to the higher mass and also for the *higher* rotational frequency (though $\Omega < \Omega_k$ but the value of Ω is sufficient to show the strong gravity frame-dragging effect) a real pulsar drags the local inertial frames of its interior spacetime with much higher rate than any other ordinary rotating object.

We calculate interior frame-dragging frequencies for some known pulsars with various EoSs considered in this article and put them in Table 3. This table also shows that the frame-dragging rate is higher at the surface of the pole than that at the surface of the equator. These values differ due to different EoSs. It could be easily seen from the plots in Figs.5-7 that the ‘peak-dip’ anomaly also appears in the cases of the real pulsars. The ‘peak’ is located around $r_{peak} \approx 0.7r_e$ and the ‘dip’ is located around $r_{dip} \approx 0.9r_e$ in our examples. For a specific pulsar, the positions of ‘dip’ and ‘peak’ do not change due to the different EoSs. Thus, we can conclude that *the positions of the ‘peak’ and the ‘dip’ are independent of EoSs for a particular pulsar.*

We can see from the Fig.8 that the value of θ'_{cr} is around 30° for the pulsar J0737-3039A for two different EoSs: DD2 and APR. Thus, we can conclude that *the value of θ_{cr} is independent of EoSs for a particular pulsar.*

5. Conclusion and Discussion

We have derived the exact frame dragging frequency inside the rotating neutron star without making any preliminary assumption on the metric components and energy-momentum tensor. We show that the frequency must depend on r and θ , it should not depend solely on its radial distance r . This formulation also helps us to predict the ‘exact’ frame-dragging frequencies for some known pulsars. We have also calculated the frame-dragging frequencies at the centers of these pulsars without imposing any boundary conditions on them. We have obtained an anomaly along the equator and its around due to the colatitude (θ) dependency of the frame-dragging effect inside the pulsars. Now, we can draw two major conclusions from our results: (1) The positions of the ‘peak’ and the ‘dip’ do not depend on the EoSs. It depends on the frequency Ω and the central density ε_c of the particular pulsar. (2) The value of the ‘critical’ angle θ_{cr} is also independent of the EoSs for a specific pulsar. We have given a proper explanation of the ‘peak’ and the ‘dip’ mathematically.

Acknowledgements: CC and KPM would like to thank Prof. Dr. Parthasarathi Majumdar for various discussions regarding this project. His comments and valuable suggestions help CC a lot to make this work more appropriate. Last but not the least, CC thanks Prof. Dr. K.D. Kokkotas of University of Tübingen,

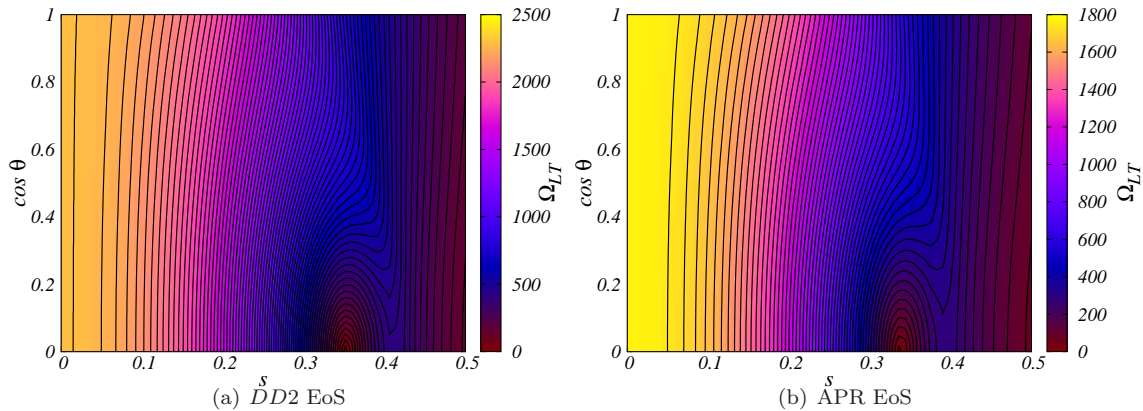


Fig. 4.— 3-D plots of Ω_{LT} of the pulsar which is rotating with $\Omega_k = 5000 \text{ s}^{-1}$ as a function of s and $\cos \theta$ for (a) DD2 EoS and (b) APR EoS.

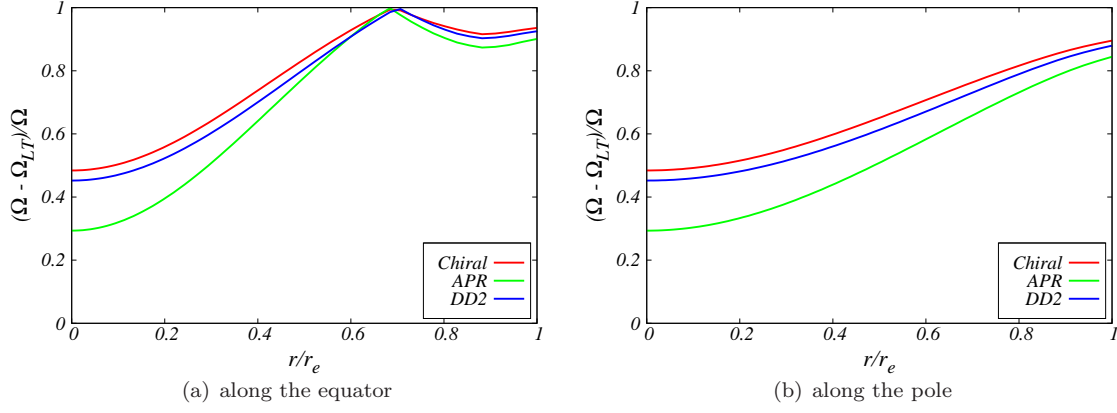


Fig. 5.— *Frame-dragging effect inside the rotating neutron star from the origin to the surface, calculated for J1807-2500B ($M = 1.366M_{\odot}$, $\Omega = 1500.935 \text{ s}^{-1}$)*

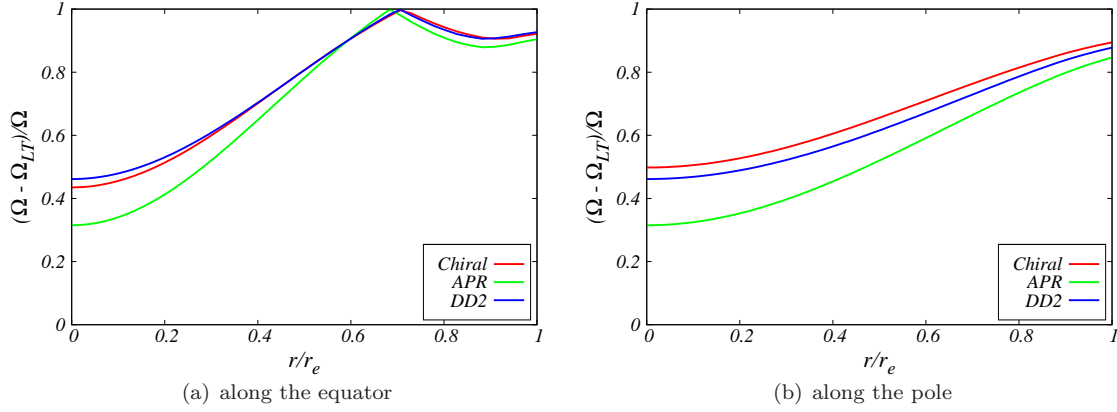


Fig. 6.— *Frame-dragging effect inside the rotating neutron star from the origin to the surface, calculated for J0737-3039A ($M = 1.337M_{\odot}$, $\Omega = 276.8 \text{ s}^{-1}$)*

Germany for gracious hospitality during an academic visit and for invaluable discussions regarding the subject of this paper. Two of us (KPM & CC) are grateful to Dept. of Atomic Energy (DAE, Govt. of India) for financial assistance.

REFERENCES

Antoniadis, J. et al. , *Science* **340**, 1233232 (2013).

| | P_k (ms) | Along the equator | | | Along the pole | | |
|--------------------|---------------|-------------------|-------|--------|----------------|-------|--------|
| | | APR | DD2 | Chiral | APR | DD2 | Chiral |
| $\tilde{\omega}_s$ | J1807-2500B | 0.099 | 0.075 | 0.064 | 0.156 | 0.120 | 0.105 |
| | J0737-3039A | 0.095 | 0.073 | 0.062 | 0.154 | 0.122 | 0.106 |
| | B1257+12 | 0.122 | 0.091 | 0.077 | 0.188 | 0.145 | 0.126 |
| $\tilde{\omega}_c$ | J1807-2500B | 0.707 | 0.548 | 0.516 | 0.707 | 0.548 | 0.516 |
| | J0737-3039A | 0.685 | 0.538 | 0.502 | 0.685 | 0.538 | 0.502 |
| | B1257+12 | 0.825 | 0.632 | 0.601 | 0.825 | 0.632 | 0.601 |

Table 3: Relative angular velocities of the local inertial frame-dragging at the surface $\tilde{\omega}_s (\equiv \omega_s/\Omega_k)$ and the centre $\tilde{\omega}_c (\equiv \omega_c/\Omega_k)$ of some known rotating neutron stars.

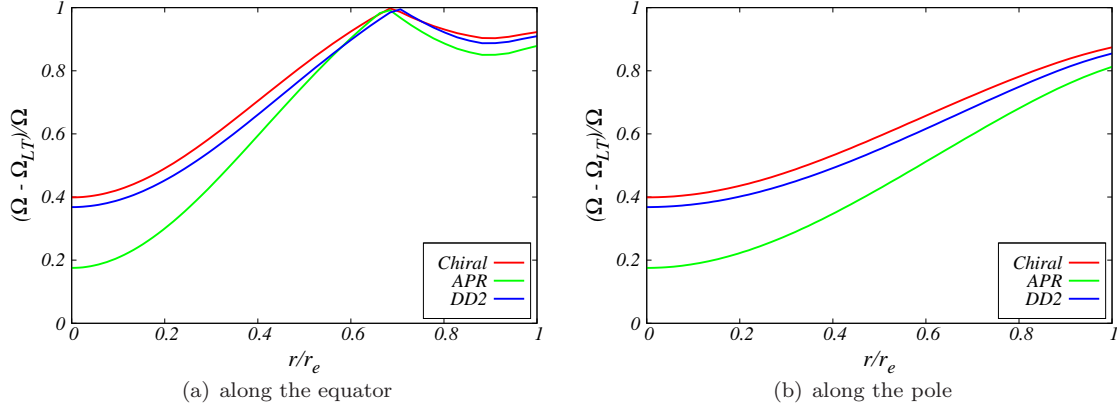


Fig. 7.— *Frame-dragging effect inside the rotating neutron star from the origin to the surface, calculated for B1257+12 ($M = 1.5M_{\odot}$, $\Omega = 1010.321 \text{ s}^{-1}$)*

Arnett, W.D., Bowers, R.L., *ApJS* **33**, 415 (1977).

Akmal, A., Pandharipande, V. R., Ravenhall, D. G., *Phys. Rev. C* **58**, 1804 (1998).

Banik, S., Matthias, H., Bandyopadhyay, D., Greiner, W., *Phys. Rev. D* **70**, 123004 (2004).

Chakraborty, C., Majumdar, P., to appear in *Class. Quantum Grav.*, arXiv:1304.6936v2 [gr-qc].

Chakraborty, C., Pradhan, P., *Eur. Phys. J. C* **73**, 2536 (2013).

Cook, G.B., Shapiro, S.L., Teukolsky, S.A., *ApJ* **398**, 203 (1992).

Hartle, J.B., *ApJ* **150**, 1005 (1967).

Hartle, J.B., *ApJ* **153**, 807 (1968).

Hartle, J. B. 2009, *Gravity: An introduction to Einstein's General relativity*, Pearson.

Hanauske, M., Zschesche, D., Pal, S., Schramm, S., Stöcker, H., Greiner, W., *Astrophys. J.* **537**, 958 (2000).

Komatsu, H., Eriguchi, Y., Hachisu, I., *MNRAS* **237**, 355 (KEH) (1989).

Stergioulas N., Friedman J.L., *ApJ* **444**, 306 (1995).

Typel, S., Röpke, G., Klähn, T., Blaschke, D., Wolter, H. H., *Phys. Rev. C* **81**, 015803 (2010).

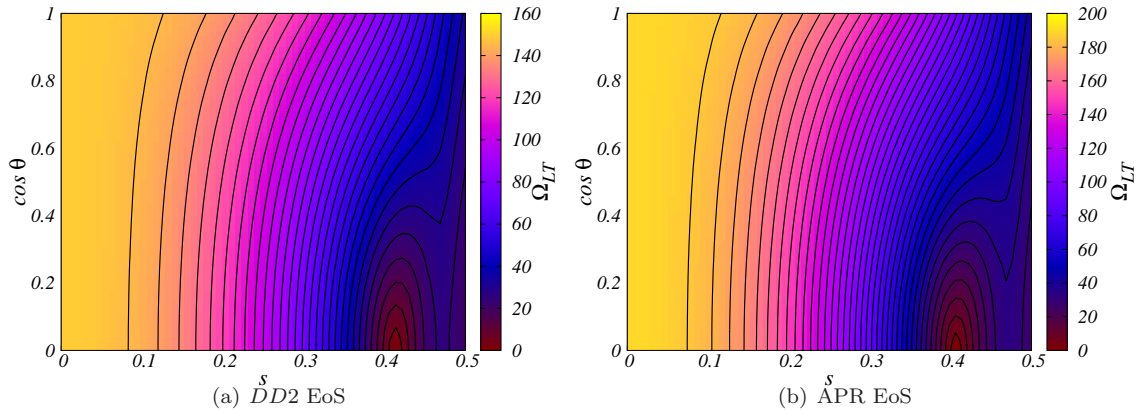


Fig. 8.— *3-D plots of Ω_{LT} of the pulsar J0737-3039A as a function of s and $\cos \theta$ for (a) DD2 EoS and (b) APR EoS*

Weber, F., *Pulsars as Astrophysical laboratories for Nuclear and Particle Physics*, IOP (1999).